Soft Matter

Accepted Manuscript

ROYAL SOCIETY OF CHEMISTRY

www.rsc.org/softmatter

Wetting-mediated collective tubulation and pearling in confined vesicular drop of DDAB solutions

Hamidou HAIDARA

Institut de Science des Matériaux de Mulhouse (IS2M), UMR 7361-CNRS/Université de Haute Alsace, 15 rue Jean Starcky 68057 Mulhouse Cedex, France.

E-mail address : hamidou.haidara@uha.fr

Summary

Whether driven by external mechanical stresses (shear flow) or induced by membrane-active peptides and/or proteins, the collective growth of tubules in membranous fluids has seldom been reported. This is so of the pearling destabilization of these membranous tubules which often requires an external activation of the shape distortion, either induced by optical tweezers, membrane-active biomolecules, or an electrical field. Here we report such events of collective tubulation and pearling destabilization in sessile drops of didodecyl-dimethylammonium bromide (DDAB) vesicular solution that are confined by a surrounding oil medium. Based on the wetting dynamics and the features of the tubulation process, we show that the growth of the tubules here relies on a mechanism of "pinning-induced pulling" from the retracting drop, rather than the classical hydrodynamic fingering instability. We show that the whole tubulation process is driven by a strong coupling between the bulk properties of the ternary (DAAB/water/oil) system, and the dynamics of wetting. Finally, we discuss the pearling destabilization of these tubules under vanishing static interface tension and quite mild tensile force arising from their pulling. We show that under those mild conditions, shape disturbances readily grow, either as pearling waves moving toward the drop-reservoir, or as Rayleigh-type peristaltic modulations. Besides revealing singular non-Rayleigh pearling modes, this work also brings new insights into the flow dynamics in membranous tubules anchored to an infinite reservoir.

Graphical contents entry

Wetting-driven collective tubulation and pearling patterns in a sessile drop of aqueous DDAB surfactant solution (3 wt %), surrounded by an alkane oil. (Color online).

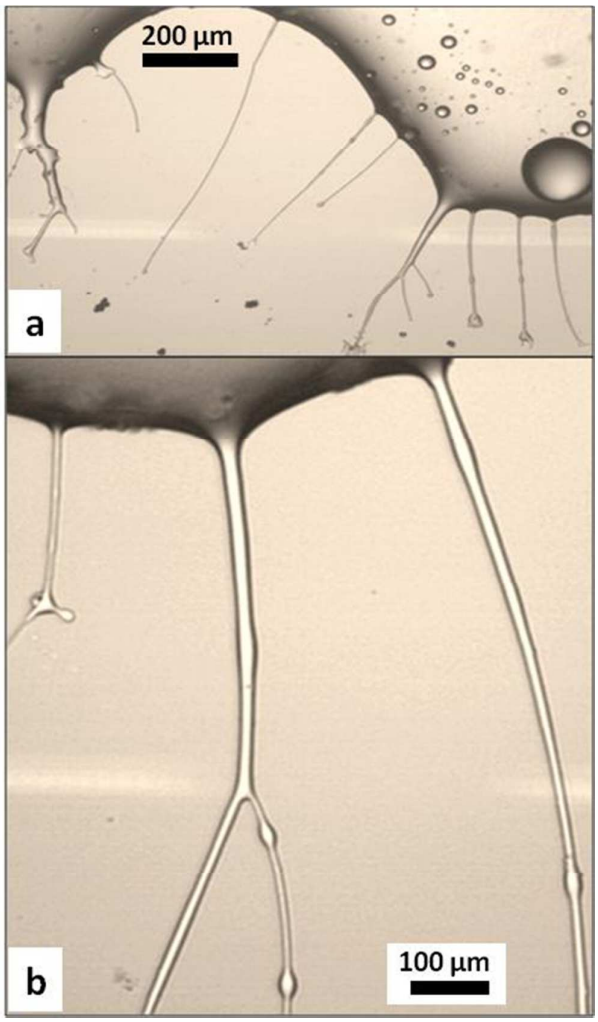

Introduction

Stress-induced tubulation of membranous fluids and objects (vesicles, cells, bilayers, lamella) or polymers, either of biochemical (peptides/proteins) or mechanical (hydrodynamic shear) origin is a rather well known and experimentally investigated phenomenon.[1-7] This is so of the pearling destabilization of these membranous tubules that has so far required the application of either a photochemical tweezer or an electrical field.[8-14] unlike falling fluid tubes, spun fibers or confined polymer threads[2] for which this instability grows spontaneously into pearling droplets. So far, the tubulation of membranous objects (cells, vesicles) has mostly involved the shear-induced extrusion and pulling of discrete tubules through capillaries,[3,4] although collective tubulation either driven by shear-flow or induced by bioactive molecules in liposomes and supported membranes has been reported.[6,7] Here, we show and explore, possibly for the first time, the occurrence of such collective tubulation event in sessile drops of aqueous didodecyl-dimethylammonium bromide (DDAB) surfactant solutions that are confined under a surrounding oil medium, in the so-called "two liquid phase" wetting configuration. Of particular interest, we show that these tubulation events are primarily driven by a strong coupling between the bulk properties (phase diagrams) of the ternary "DDAB/water/oil" system on the one hand, and the interface (wetting) behavior of the confined aqueous DDAB drop on the other hand. Beyond the structural complexity of these systems containing both lamella and vesicles, we show that the tubules here grow collectively through a "pinning-induced pulling" process of fibrillar fingers from the retracting contact line, based on the features of the tubulation (point-pinning, pulling kinetics, randomness and side-branching mode of the tubules), at the difference of classical hydrodynamic fingering instabilities of advancing wetting fronts.[15-19] Besides that wetting-driven collective tubulation, we show that the tubules that form can develop shape instability under *unusually* quite mild conditions, as compared to most reported studies where external disturbance sources (mechanical, photochemical tweezers, membrane-active molecules, electrical field)[2,8-14] are required to overcome membrane bending rigidity, and induce the shape instability. Indeed, the pearling instabilities here develop within the microtubules under vanishing static interface tension and residual tensile stress induced by their pulling from the reservoir drop to which they remain anchored. Depending on the structure of the tubules (size, membrane rigidity, internal fluid viscosity) and their anchoring to the substrate, the shape instabilities of the microtubules are shown to develop through pearling modes and patterns that here present at least two distinctive and possibly unrevealed features. The first of these features is the occurrence of moving pearls which, at the difference of the propagating "pearling front"

analytically described by Powers *et al.*,[12] do not break up into sequential daughter droplets. Instead, these pearls keep moving as a whole, along and with the tubule, to eventually re-enter the macroscopic drop (complete suction), driven by the relaxing tensile energy of pulling. The second distinctive feature of this pearling destabilization is the growth of the instability into a single or a few pearl-waves that are more or less stationary, with characteristic features (pearl radius and period) that deviate from those expected from the classical Rayleigh destabilization theory.[20] It is worth noting here that since the marginal stability analysis by Powers *et al.*[12] based on the reference works of Bar-Ziv *et al.*[9,10] on laser induced pearling of membranous tubules, very few evidence toward topological transitions of pearling patterns in these systems have been reported experimentally. The following deals, principally through a phenomenological approach, with this collective tubulation process and the related singular pearling modes that should contribute better understanding the still open issue of fluid dynamics in membranous microtubules.

Experimental

Materials

Didodecyldimethylammonium bromide (DDAB), a model synthetic double-chain surfactant[21-25] that easily forms unilamellar and multilamellar vesicles (ULV and MLV respectively)[21-25] at low concentration in water (DDAB/W) was used for all experiments. In this dilute regime where the solution lies within the first lamellar ($L_{\alpha 1}$) domain of the DDAB/W phase diagram, two concentrations were used for the dependence of the tubulation and pearling destabilization on DDAB concentration and viscosity: 3g/L~0.3 wt% and 15g/L~1.5 wt%. These two concentrations were prepared in 25 mL glass vials by adding, respectively, 60 mg and 300 mg of DDAB to 20 mL of reverse osmosis (Milli-Q) water warmed to ~50°C. This mixture was first gently shaken manually and then sonicated for a few minutes in a Branson ultrasonic cleaner (model 1050E-MTH). At these low concentrations, DDAB easily dilutes in water to spontaneously form unilamellar and multilamellar vesicles (see Fig. 1). This solution was stored at 20±0.1°C, 55% RH for 1 day before the first use, and between uses over a maximum of one week. The DDAB of analytical grade (purum) was from Fluka and used as received. For experiments involving the deposition of DDAB solution drops under oil, here referred to as "under-oil" experiments, analytical grade dodecane (C_{12}), hexadecane (C_{16}), and squalane (C_{30}) from Aldrich, and a (C_{12}-C_{16}) mixture at 50% vol. were used.

For all experiments, the reference wetting/drying experiment in air and "under-oil" tubulation experiments, 2x2 cm^2 pieces of (100) oriented 380 µm thick single side polished silicon

wafers (Si) bearing their native oxide (~2 nm) were used as substrates. Prior to wetting experiments, these pieces were cleaned by sonication in warm (45°C) chloroform for 10 minutes and dried under nitrogen flow, after we showed that this cleaning process producing a reference water contact angle θ_w ~ 50° in air, also produces the optimal "under-oil" wetting conditions leading to tubulation.

Experimental procedure

For the reference wetting experiment in air, a drop of ~10 µL was deposited on the substrate and left to freely evolve through spreading and evaporation-drying. For "under-oil" tubulation experiments, the substrate was placed in a glass cell (0.8 cm height and 4 cm diameter) containing the oil over 0.7 cm thickness. Before the deposition of the aqueous suspension drop, the whole system was placed under a video-microscope interfaced with a computer and a video acquisition software (Open Box Ver. 1.8) for images and video acquisition. The video-microscope comprises an Olympus BX 60 optical microscope equipped with a DIC (differential interference contrast) device, and a COHU solid state CCD camera operating at 25 images/s. After a gentle agitation of the stock solution, ~10 µL DDAB suspension drop was equally gently deposited, and the wetting dynamics followed or recorded, starting with a 5x magnification long working distance objective. Depending on which dynamics and/or phenomenon is observed (dewetting/fragmentation of the drop, tubulation and pearling), two other objectives (magnification of 10 and 50, long working distance) have been used. All the experiments were performed under usual laboratory conditions of 22±1° C and 40±5% RH.

The images are either captured individually during the dynamics or extracted from recorded movies using VirtualDub (1.9.11) and ImageJ (1.47d) free software. Image analysis for the size measurement, the growth kinetics and migration velocities ("displacement vs. time") of the structures (tubules and pearls) are performed using ImageJ, after setting length scales for all images, from pixels to metric units (µm).

Results and Discussion

Reference wetting experiment in air

Fig. 1 shows a typical result of the preliminary reference wetting experiment of a dilute DDAB suspension drop in air, respectively in the early stage of its deposition (Fig. 1a) and the late stage of its evaporation-drying (Fig. 1b), on the cleaned silicon substrate. Besides ascertaining the presence of large vesicles by the dense aggregation networks that they form in the late drying stage, Fig. 1 also reveals the formation of long and large threadlike-to-tubular structures, possibly from collapsed and merging vesicles and lamella within the

confined border of the evaporating drop. The intuition that preventing the evaporation-drying of the drop by placing it under oil, while maintaining similar spreading and edge confinement that allow the above structural transitions is at the basis of the present work and following sections.

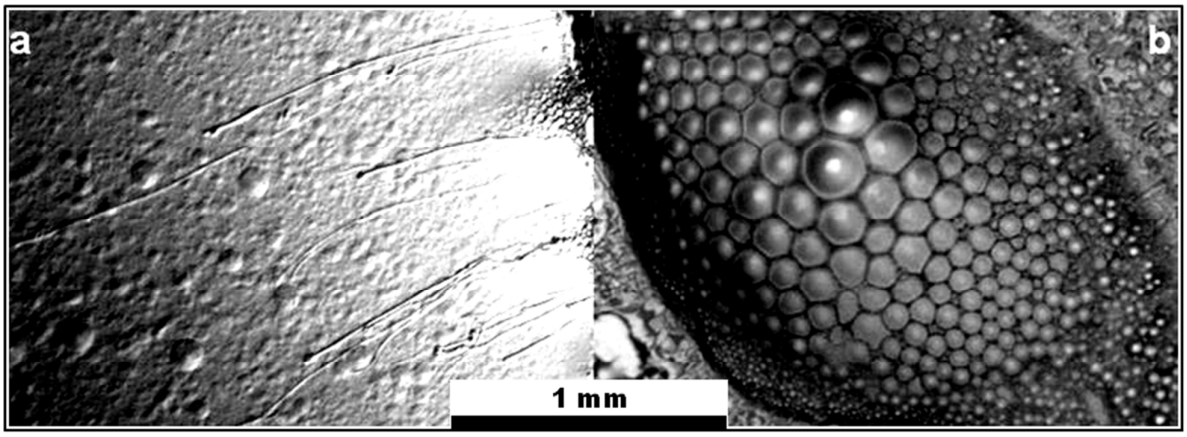

Figure 1: Evaporation-drying of a DDAB vesicle solution drop at 0.3 wt% on Si wafer in air: **a**) early to mid-stage of the evaporation-drying, with threadlike to filamentous vesicles developing and extending from the confined edge of the drop; **b**) collected vesicles network at the center of the drop in the very late drying stage. The contact angles in **a**), right after spreading and on receding are both < 10° on the cleaned Si wafers in chloroform, under sonication.

Under-oil wetting and tubules growth

The results shown in Figures 2a-to-2f are representative of the early stage wetting dynamics observed in "under-oil" wetting experiments, although these dynamic events (dewetting and fragmentation of DDAB drop) are strongly modulated by the chain length and viscosity of the surrounding alkane oil. These results are represented here for squalane (C_{30}) and hexadecane (C_{16}), two oils were purposely chosen for their viscosity which allows capturing the early stage wetting behavior of the confined DDAB drop by damping the flow instability and fragmentation of the drop (Fig. 2), making easier the observation of the early stage wetting events, contrary to dodecane (C_{12}) oil. Clearly, what Fig. 2 shows is the remarkable difference in the wetting behavior of the confined DDAB drop, depending on the size (chain length) and viscosity of the surrounding oil. Under hexadecane, this is characterized at the drop center by a much higher density of dewetting and fragmentation holes (Fig. 2a) that remain in addition definitely filled by the oil (Fig. 2b-c). Under squalane the drop which spreads slowly with a reduced equilibrium extent only shows a few (if any) dewetting holes (Fig.2d) that are here completely refilled (Fig. 2e-f) by the back flow of the DDAB drop (healing of the dewetting holes). One can account at least partly for this oil-dependent behavior of the confined DDAB drop by the bulk properties of ternary (oil/water/DDAB) systems that have been extensively

studied.[22,23] Indeed as shown for these ternary DDAB/W/oil phase diagrams, n-alkane oils, and particularly short chain alkanes (n≤14) have a higher penetration in DDAB/W mixtures,[23] accounting for the microstructural variety of the ternary mixtures. In our system (Si supported vesicular drop under oil), we found that the same bulk properties were effective, driving a more or less rapid and strong destabilization of the drop upon its deposition, through dewetting and fragmentation (Fig. 2). As expected from the length dependence of the penetration rate (miscibility) of the n-alkanes,[22,23] we showed that the strength of that penetration significantly increases from C_{30} to C_{12}, using squalane (C_{30}), hexadecane (C_{16}) and dodecane (C_{12}), with a dewetting and fragmentation of the drop which are quite instantaneous and more violent for shorter chain alkanes (Fig. 2a-to-2c, vs. 2d-to-2f). This dewetting/fragmentation process, which develops mostly around the center of the highly spread and thinned drop, driven by the penetration of the surrounding oil creates an outward pressure wave, $P_{outward}$, that further pushes and forces the spreading of the preserved rim-like drop. This forced outward displacement may be increased by the hydrostatic pressure $\Delta\rho_{(oil/solution)}gh_{drop}$ over the confined drop (or rim) of thickness h_{drop}, although this term of negligible and comparable magnitude for hexadecane and squalane cannot account for the observed drastic difference between these oils regarding the tubulation process. As is visible in (Fig. 2d-to-2f), in the surrounding C_{30} oil of higher viscosity, the initial events of dewetting and fragmentation of the confined drop lead to the formation of a thick pressurized rim that also takes more time to relax. Indeed, as compared to C_{12} and C_{16}, the viscous damping in C_{30} strongly slows down the outward displacement of the rim (drop edge), the velocity of which at first order in the surrounding oil viscosity η_{alkane} is,[26] $V_{rim}\sim(P_{outward}.d/\eta_{alkane})$, where d stands for the characteristic size of the flow diffusion layer in the surrounding oil. As a result, the rim which is compressed by the outward pressure while relaxing ahead very slowly rather protrudes to form a thicker rim. For this long C_{30} alkane (and to a lesser extent for C_{16}), the rim slowly relaxes with a characteristic timescale $\sim(\eta_{alkane}/P_{outward})$ from the end of the dewetting/fragmentation event, with no noticeable retraction. For C_{12} and for C_{16} on the other hand, as the pressurized drop edge relaxes, which lasts from a few tens of seconds, the spreading ceases and the rim-like border begins to recede, revealing tubules that are pulled from the drop edge, as Fig. 3a-3b, Fig. 4a-to-4c and Supplementary information S1 and S2 show it for both C_{12}, (C_{12}-C_{16}) mixture and C_{16} systems. In this respect, it is worth noting that a primary requirement for the growth of the tubules is that the drop retracts, more or less significantly, after the excess spreading induced by the outward pressure (flow) that follows

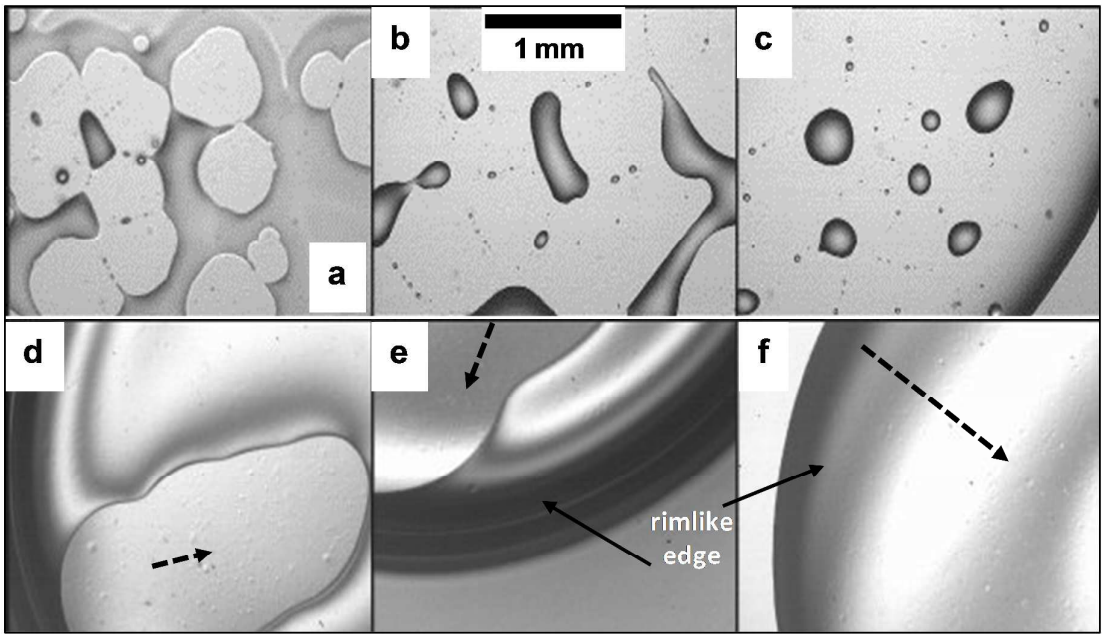

Figure 2: Evolution of the confined DDAB solution drops (0.3 wt%) upon deposition under hexadecane (from **a** to **c**), and squalane (from **d** to **f**). Under hexadecane, the early spreading is accompanied by a dewetting and fragmentation in the center of the drop that creates a high density of holes (**2a**) which remain definitely filled by the hexadecane (**2b-c**). Note in this case (**2c**) that some of the fragments of the aqueous DDAB drop stand inside the surrounding oil as microemulsion-like droplets. Under squalane the drop spreads slowly with a reduced equilibrium extent showing only a few (if any) dewetting holes (arrow in **2d**) that are slowly refilled (arrows in **2e-f**) by the back flow/receding of the drop (healing of the dewetted holes); **e**) partially refilled hole, **f**) complete refilling and recovering of the drop shape.

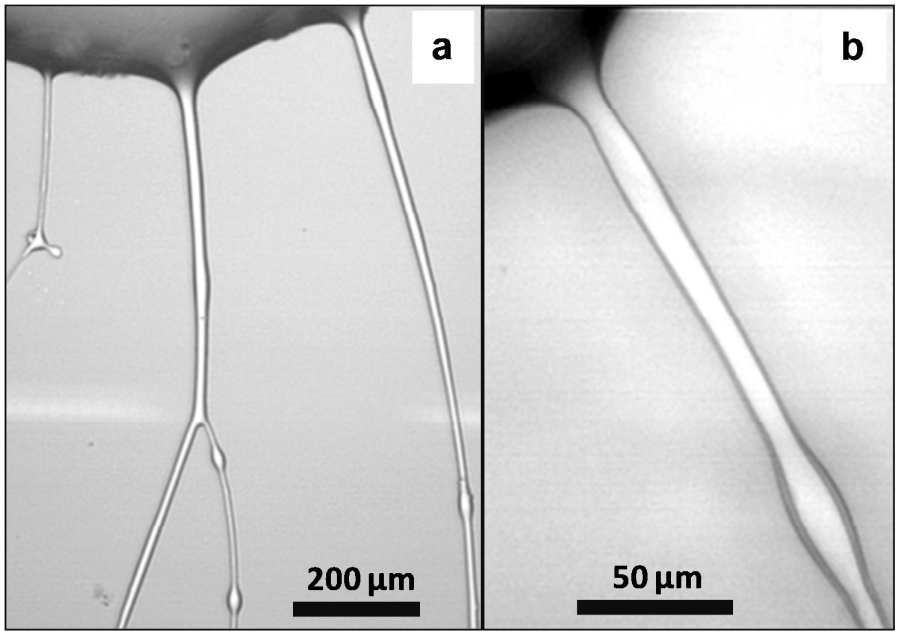

Figure 3: Tubulation front and tubules fine structure shown for a DDAB solution drop (0.3 wt%), respectively, **a**) in 50 vol.% (C_{12}-C_{16}) mixture, and **b**) in C_{12} where a single tubule was captured at a resolution showing the wall structure of the membranous tubule on a growing pearl (bulge).

its deposition. As shown in Fig. 3 and Figs. 4a-4c, the pulling and growth of the tubules also require anchoring points which may either be embedded in the drop as emulsion-like droplets, or come from the surface as dust particles visible at some tubules extremities (see S1 and S2), or from topographical or chemical defects on the surface[27] as this is possibly the case in Fig. 4a-c. Though both types of surface defects (topographic and chemical) are supposed to exist a priori on the substrate, random chemical defects arising from the non-homogeneous removal of organic contaminants by solvent cleaning (see experiment section) are more probable candidates on the polished Si substrates of nanoscale roughness. As the contact line (CL) slowly recedes, the membranous tubules (see fine tubule structure in Fig. 3b) that are henceforth anchored by these point-defects at their external extremity are further pulled out from the rim. Although we could not access the early stage of the formation of the tubules within the confined drop edge, it is likely that this tubulation process can take place from either of the three following structures : 1) the embedded threadlike vesicles similar to those visible in air-dried drops (Fig. 1a), 2) the microemulsion-like droplets (Fig.2c) resulting from the dewetting/fragmentation of the DDAB drop, and that sit on the substrate, surrounded by the oil (Fig.2c), or 3) the membranous DDAB layer that coats the interface of the rim-like drop with the surrounding oil. Indeed, the pulling of the embedded threadlike vesicles or the shear-induced threading of microemulsion-like droplets within the retracting drop edge, through the DDAB layer coating the (drop/oil) interface can both lead to the observed tubulation process. Similarly, the direct pulling of the interface DDAB layer coating the receding rim-like drop and enclosing the aqueous DDAB solution can equally lead to the observed tubulation process, although some of our microscopy images strongly suggest either of the first two processes (see Fig. 5 and caption later in the text). Finally, regardless of the nature of the pinning-defects (surface defects[27] or drop-embedded objects), the features of this tubulation process (visible pinning points, pulling of tubules visible only on retraction, random tubules distribution, side-branching mode of tubules) clearly point to a "pinning-induced pulling" process, rather than a classical hydrodynamic fingering instability. Indeed, although most of fingering structures formed at wetting fronts arise from digitation instabilities which are of purely dynamical nature and virtually independent of pinning-defects, fingering process based on the pinning-induced pulling of fluid segments[28] or macromolecules by retracting contact line is known for a long time and used as a technological patterning tool (stretching of DNA strands for instance).[29-31] Beside the fact that they are observed under forced wetting/flow conditions (spinning drop, inclined substrate, pressure, density, thermal gradients), an essential feature of hydrodynamic fingering

instabilities is that they have a characteristic and predictable wavelength, regardless of the nature of the gradient that drives them.[15-19] A second important feature of these hydrodynamic instabilities is that they systematically occur on spreading, ahead of the advancing front, but seldom, if not never on receding, as attested by the literature. [15-19] Furthermore, when taking place in wetting films, these hydrodynamic fingering instabilities have been shown to arise from a thickening of the advancing front, the destabilization of which thickened front creates the fingers.[16,17,19] Incidentally, the thickest moving drop fronts that form under squalane in our experiments (Fig.2d-e-f) never lead to any fingering or tubulation instability. And even when observed with surfactant-like solutions where it is driven by Marangoni flow, this hydrodynamic fingering instability occurs systematically on spreading, forming in that case tree-like fractal fingers protruding ahead of the apparent contact line,[32] instead of well-defined discrete tubules. Similarly, Rayleigh-Taylor (gravity) and Saffmann-Taylor (viscous) instabilities which also develop on advancing fluid/fluid fronts are characterized by fingering patterns of predictable and well defined wavelengths and shapes,[18,33] as shown by Hele-Shaw cell experiments. Finally, while none of the above features of purely hydrodynamic-driven fingering is observed in our study, our experiments clearly show the growth of the tubules, exclusively on *retraction* of the wetting front, supporting a tubulation mechanism based on a "pinning-induced pulling" process.[28-31]

It is worth recalling here that the above results were all observed on cleaned Si substrates (see experimental), letting open the question of how far these "under-oil" wetting dynamics and related tubulation are influenced by the surface? This question was at least partially answered by the complementary "under-oil" experiments we performed on both as-received (non-cleaned) silicon wafers of reference water contact angle θ_w~68°±3, and hydrophobized substrate (methyl-terminated hexadecyltrichlorosilane monolayer coated silicon)[26] of water contact angle θ_w~105°±2. Indeed, whilst tubulation was observed on the as-received Si wafer, though with less reproducibility compared to solvent cleaned wafer, no tubulation was observed on the hydrophobized Si wafer. Furthermore, neither the early stage dynamic instabilities (dewetting, fragmentation of the confined DDAB drop…) nor a retraction of the drop front were observed on the hydrophobized substrate. Instead, on deposition of the DDAB drop on the hydrophobized surface, a fast and strong spreading develops, thinning instantly and strongly the drop. Most importantly, unlike non-cleaned and solvent cleaned Si wafers, this fast and strong spreading drives on the hydrophobized substrate the well-known hydrodynamic fingering instability,[32] with very dense treelike fingers propagating ahead of the spreading front (Supplementary Information S3). The surface state and wetting of the

substrate therefore influence the whole "under-oil" wetting dynamics and tubulation process, although more systematic studies would be required to better understand and described this influence, beyond the sole effect of surface defects.

Once the tubules are pulled from the receding drop edge, they lie under the alkane oil either as unperturbed tubule segments or as pearls necklace upon fragmentation, as shown in Fig. 3 and Fig. 4a-to-c. For reason of interface energy minimization, this requires that the outer layer of the tubule exposes the double-alkyl chains of the DDAB surfactant to the surrounding alkane oil. As a result, the membranes of tubule should have an odd number of layers (1, 3...), regardless of whether they are pulled from the interfacial DDAB layer that coats the receding rim-like drop, or from the drop embedded threadlike vesicles. It is worth noting in this regard that the vanishing equilibrium interface tension of ~10^{-4} N/m reported in the literature[34] and ~10^{-3} N/m measured in this work between the aqueous DDAB solution (1.5 wt%) and hexadecane by the Wilhelmy plate tensiometry well supports that interface free energy minimization.

Beyond the growth of the tubules from the drop reservoir and their high peripheral density, this wetting-assisted tubulation also reveals structural features (side-branching) that are ubiquitous of crystallization/solidification and fractal growth in general. As Fig. 3a and Fig. 4b to 4c show it, bifurcation-like side branches appear along primary tubules at many places. But unlike standard bifurcation or tip-split branching in growing crystals or moving fluids fronts that are either driven by interface energy or pressure fluctuations, the branching here results simply from the merging of two tubules that grow at locations that are close enough on the rim. At the crossing point of the growth directions of these non-parallel tubules, they merge into thicker "root-tubules" that keep growing as the CL recedes, as schematically depicted in Fig. 4d. This side-branch formation based on "tips-merging" is a much less often observed process as compared to the classical bifurcation (tip-splitting) that develops in an opposite direction.

Pearling instabilities and structures

For the conditions of our experiments where the tubules are formed in dilute DDAB solutions drops, under low viscosity alkane oils (C_{12},C_{16}), the tubules evolve essentially through three paths which are determined by the balance between their pinning strength at the anchored extremity W_P, and the tension σ arising from their pulling out of the drop border. These scenarios also determine with the DDAB concentration the average lifetime of the tubules from a few minutes to hours, from their growth to complete pearling fragmentation and

subsequent deliquescence of the resulting droplets. Although irrelevant regarding the pearling phenomenon, one of these tubule evolution paths is that in which the tubule starts to retract in the early stage of the growth and re-enter the drop before pearling, driven by the relaxing

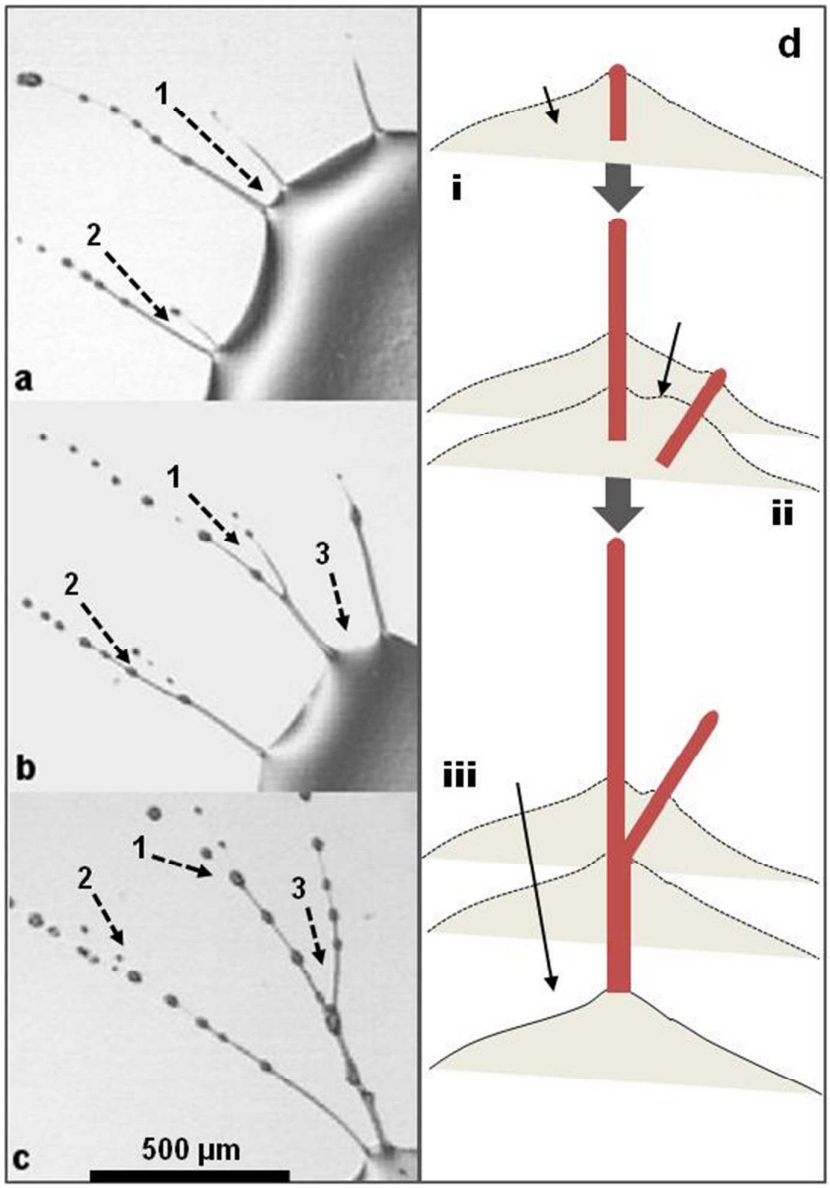

Figure 4: Panels **a**)-**b**) and **c**) show a characteristic growth sequence of the membranous tubules along the receding contact line of the aqueous DDAB vesicular drop (0.3 wt%) under hexadecane, along with the corresponding patterns of pearls arrays. The arrows (1, 2 and 3) indicate from **a**) to **c**) locations where a branching between the growing tubules takes place as they merge. The formation of these branching patterns by a "tips-merging" process, vs. standard tip-splitting is schematically drawn in **d**).

tensile stress $\sigma > W_P$ (depinning), and the pressure gradient ∇P between the tubule and the drop reservoir. For all these retracting tubules that re-enter the drop, the tubule contraction rate V_{TC} and the local receding velocity of the drop edge V_D are such as $V_{TC} > V_D$.

The two last cases are the relevant tubule evolution dynamics that are hereafter considered for pearling instabilities. In both cases, the tubules grow proportionally to the local receding velocity of the drop (i.e. as $\sim V_D.t$) over timescales that are beyond the early stage (Supplementary Information S1, S2). However, they differ in their long-term behavior that determines their pearling mode. In the first case, the tubules keep growing between the pinning (anchoring) point and the drop reservoir until the receding stops, and along with the growth of the tubule the pearling process also develops concomitantly, leading generally to stationary pearls. This case requires that the tubule be firmly anchored at its pinned extremity and therefore, a balance of tension and pinning satisfying $\sigma < W_P$. In the second case, the tubule is unpinned or broken at its anchoring point, either before the receding has stopped or shortly after, leading to a combined pearling and global tubule suction toward the drop reservoir. For this latter case, the balance between the pulling tension and the pinning strength (respectively tubule cohesion) should be such as $\sigma \geq W_P$ at a certain time of the pulling to observe the depinning and global tubule retraction. The following is a phenomenological description of these rather unusual pearling dynamics along membranous tubules that are either stretched between the pulling drop reservoir and the defect pinning point, or retracting from their free end (upon depinning) towards the reservoir.

From a theoretical standpoint, the growth of an undulatory shape disturbance in an initially uniform, cylinder-shaped membranous tubule requires at leading order that the bending rigidity be balanced by the tension along the tubule (capillary and externally exerted). Keeping these leading order terms in bending rigidity and tension, the free energy of the tubule of unperturbed radius R_t and length L_t is thus written,

$$\boldsymbol{E} \cong (\kappa_B/2R_t^2 + \gamma_{interf})A - f.L_t \qquad (1)$$

where κ_B is the bending modulus, γ_{interf} the static interface tension, $\boldsymbol{f}$ the tensile force of pulling from the drop reservoir, and $A=2\pi R_t L_t$ the area of the membranous tubule. As Fig. 4 and the Supplementary Information S1, S2 show it, the pearling instability grows concomitantly to the pulling in most cases, meaning that the volume of the destabilizing tubules is not conserved. The minimization of $\boldsymbol{E}$ with respect to R_t and then L_t in eq. 1 gives a pulling tensile force $\boldsymbol{f} = (2\pi\kappa_B/R_t)$, an interface tension $\gamma_{interf} \sim (\kappa_B/2R_t^2)$, and an equilibrium relation for the stretched tubule,[14]

$$T^* = (2\pi\kappa_B/R_t)+2\gamma_{interf}R_t = (1+2\pi)(\kappa_B/R_t) \quad (2)$$

where T^* stands for the apparent tubule tension. No matter from which of the embedded threadlike vesicles or shear-threaded microemulsion-like droplets the tubules are pulled from, the first term of the apparent tension can be related and roughly computed from the viscous shear exerted on the tubule at the conical pulling border (see Fig. 3) as,

$$2\pi\kappa_B/R_t \cong (\eta_{sol}+\eta_{oil})\boldsymbol{l}V_t \quad (3)$$

η_{sol} and η_{oil} are, respectively, the viscosity of the aqueous DDAB solution and surrounding oil, V_t the average pulling rate of the tubule, and $\boldsymbol{l}$ the length of the pulling cone. This gives an estimate of the bending modulus of the tubule,

$$\kappa_B = (R_t/2\pi)(\eta_{sol}+\eta_{oil})\boldsymbol{l}V_t \quad (4)$$

Using quoted values of η_{oil} ~3.10^{-3} Pas for C_{16} and η_{sol} ~ $1.5x10^{-3}$ Pas for both concentrations of 0.3 and 1.5 wt% DDAB,[25,35] a tubule radius R_t = 5 µm, a size of the pulling cone $\boldsymbol{l}$ =70 µm and a pulling velocity V_t = 0.2 µm/s determined from experiments shown in Fig. 5A (1.5 wt% DDAB), a bending modulus κ_B ~$1.5x10^{-19}$ J was estimated, an order of magnitude which is typical of double-tail surfactants bilayers. Let us note that this estimate is of course compatible with the above discussed criterion of interfacial free energy minimization of the tubule, which requires an odd number (likely 3) of layers in its membrane exposed to alkane medium. Indeed, estimated bending rigidities of unilamellar and multilamellar vesicles give values (5-10k_BT and 10-15k_BT, respectively)[36] which are close enough, while covering the above estimated value of $1.5x10^{-19}$ J for tubules with membranes likely consisting of 3 DDAB layers.

Whether the pearls are stationary or moving, the pearling destabilization is driven here by these two competing curvature and tension terms which set the threshold for the shape destabilization of the stretched tubule. But besides the above and rather reasonable estimates, what this tubulation process here shows is that even under vanishingly low tensions, static interface (γ_{interf}) and exerted pulling ($\boldsymbol{f}$) tensions, pearling destabilization well develops along these membranous tubules, as discussed further in the following.

Pearling on stretched tubules

Fig. 5A show the sequence of tubulation and pearling in a 1.5 wt% DDAB drop under (C_{12}-C_{16}) mixture for which tubules remain stretched between the reservoir and the anchoring point during the pearling process. The sequence of Fig. 5A shows the time-growth of the tubules along with the pearling instability, leading to a sequence of stationary pearls along the stretched tubule, as is remarkably more visible on the main tubule branches on Fig. 4. The dynamics was captured over 24 hours, long after the whole system was completely stabilized and morphologically turned to gel-like fluid after swelling (Fig. 5B). *(Incidentally these panels of Fig. 5B show at both magnifications a morphology of the pulling zone that strongly suggests that the tubules may form from drop-embedded structures (threadlike-vesicles, microemulsion-like droplets), as already hypothesized earlier in the paper).* As this can be seen from Fig. 5 (and Fig. 4 too), the growth of the pearls occur only for a characteristic pulled length of the tubule which depends on the tubule radius and tension, and sets the period (wavelength) of the pearling sequence. Within the frame of Rayleigh-type capillary instability,[20] one expects pearling patterns with a wavelength λ scaling as (λ/R_t) ~9, and a pearl size (radius) of order R_{pearl} ~$2R_t$, R_t being the unperturbed tubule radius. The freshly formed patterns in Fig. 5 (5A, 90 min.) have average pearling periods (λ/R_t) ~30, and pearl sizes R_{pearl} ~$4R_t$, which notably deviate from those expected for a classical Rayleigh-Plateau pearling event, although the former was shifted downward to (λ/R_t)~15 by the swelling of the pattern at longer time (Fig. 5B). In contrast, Fig. 4 which also shows pearling patterns characterized by a sequence of stationary pearls along tubules that remain stretched rather displays average pearling period (λ/R_t) ~10, and pearl size R_{pearl} ~$3R_t$ that are much close to those expected for a Rayleigh pearling instability. These results thus suggest a dependence of both the pearl density and the characteristic features of the pearling pattern (λ and R_{pearl} vs. R_t) on the DDAB concentration, although this needs to be further formalized through a more systematic concentration-dependent study, keeping identical the surrounding alkane oil. On the other hand, these results definitely show that whatever the (two) DDAB concentration or the surrounding oil (C_{12}, C_{12}-C_{16} mix, C_{16}), the pearling period along those tubules that remain stretched is not constant here, but increases in average toward the reservoir, possibly with the pulling tension and the size of the residual tubule being pulled out (Fig. 5 and Fig. 4). To our knowledge, this dilation of the pearling period along membranous tubules that are being pulled out from a reservoir is all but trivial. Indeed, this result which accounts for a generally expected dependence of the pearling features (λ, R_{pearl}) on the size of the tubule, for constant size tubules (L_t and R_t) and tension, is here recovered under dynamical conditions, for a

stretched tubule of variable residual size and pulling tension. This result too in particular would deserve more systematic concentration-dependent investigations in future developments of these works.

Aside these stationary pearls that develop on fully stretched tubules as observed mostly with DDAB drops of 1.5 wt% (slightly more viscous), these pearling events also involve pearls that move and coalesce along "globally" retracting tubules. These pearling events that occur mostly with 0.3 w% DDAB solutions are described below.

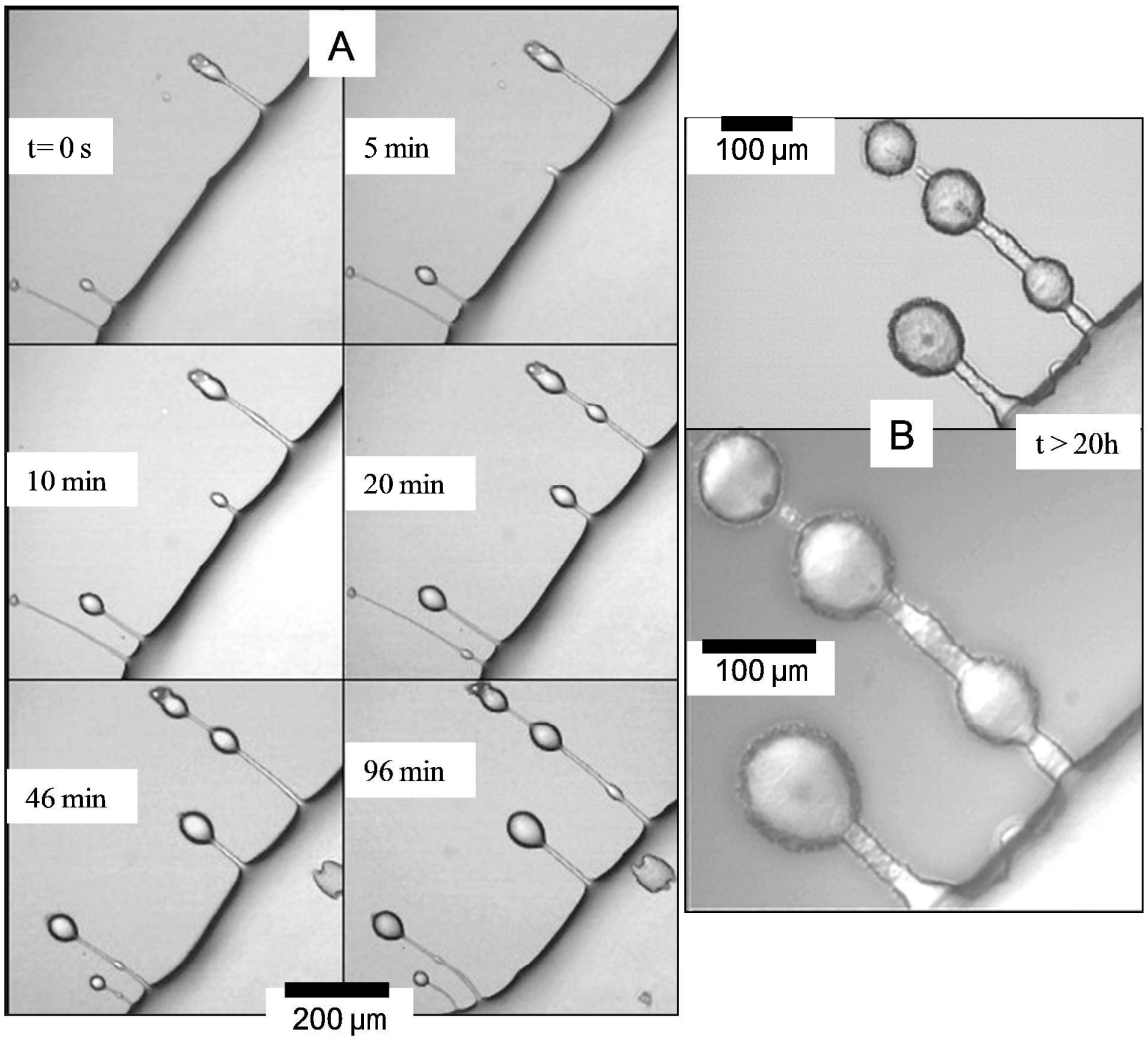

Figure 5: Time-growth of the tubules and pearling instability in 1.5 wt% DDAB drop under 50 vol.% alkane oil mixture (C_{12}-C_{16}), a case where the tubules remain attached and stretched between their anchoring points during the whole dynamics. **Panels A** represent the growth sequence from t = 0 to the complete arrest of the pulling (receding) front at t = 96 minutes (1h36min). **Panels B** correspond to the same tubules and pearling patterns at a higher magnification, after 20 hours aging and a swelling-induced morphological reconstruction. These last panels visibly suggest a continuation of the tubule by drop embedded structures that cross the pulling border and go beyond.

Pearling on retracting tubules

Propagating "pearling front" involving the continuous motion of a unique pearl wave from one extremity of the tubule, without breaking into sequential daughter drops is known and described in the litterature.[12] At the difference of this propagating "pearling front", the pearling process we here describe is a global or sequential motion of the pearls that migrate and coalesce along the tube before re-entering the drop reservoir, leading eventually to the complete suction of the tubule. **Fig. 6** illustrates such pearling dynamics and its kinetic evolution for 0.3 wt% aqueous DDAB drop, under C_{12}. The directed motion of the pearls along the globally retracting tubules towards the drop is driven by the pressure gradient between the drop reservoir and the adjoining tubule segment ($P_{tubule} > P_{drop\text{-}rim}$), the restoring tensile force (eq.(2)) of the tubule after depinning or rupture, and the main drag force on the retracting tubule and moving pearls arising from the surrounding oil. The migration velocity was determined in Fig. 6b for three pearls, from the "displacement, vs. time" snapshots given in Fig. 6a. As in most observed cases, the first pearl in contact with the rim remains *virtually* stagnant up to the end of the migration process where it generally merges with the last moving pearl ($|V_1|$ in Fig. 6b), before emptying eventually in the drop. For the two other pearls, the measured velocities are comparable and of the order of 0.8 $\mu m.s^{-1}$. An estimate of this migration velocity can also be derived from a balance of the above three forces that drive the motion of the pearls along the globally retracting tubules.

$$F_{driving} \sim \pi(R_t)^2\Delta P + 2\pi\kappa_B/R_t \quad (5)$$

$$F_{drag} \sim \eta_{oil}R_t V_t \quad (6)$$

$$V_{pearl/tubule} \sim \pi(R_t^2\Delta P+\kappa_B/R_t)/\eta_{oil}R_t \quad (7)$$

In eq.(5), the pressure difference ΔP is solely related to that of Laplace capillary pressures $\Delta P_c \sim \gamma^*_{oil/tubule}(1/R_t\text{-}1/R_{rim})$, although the involved effective radius of the rim at drop edge is hardly accessible here in the system configuration. But since $R_{rim} >> R_t$, the driving pressure for the "bulb/tubule" motion finally amounts at first order to $\Delta P_c \sim \gamma^*_{oil/sol}(R_t)^{-1}$.

Using the average tubule and pearl radii R_{tub} (~3±1 µm) and R_{pearl} (~7±2 µm) for this system (Fig. 6), a driving pressure of the tubule and pearl suction $\Delta P \approx 100$ mPa between the rim and the adjoining tubule segment was found from equating the measured velocity of ~0.75 $\mu m.s^{-1}$ (Fig. 6b) to the expected one [eq. (7)]. Then equating ΔP_c above to this estimated driving pressure gradient $\Delta P \approx 100.10^{-3}$ Pa, one arrives to a value of the (tubule/oil) interface

tension, $\gamma^*_{oil/tubule}$ ~3.10^{-4} mN/m, a value which is of the order of the one that can be derived from the minimization relation (eqs.1-2), $\gamma_{interf} \sim (\kappa_B/2R_t^2) \sim 10^{-6}$ mN/m. Although negligibly small when compared to our experimentally measured static interface of 1 mN/m (10^4 order of magnitude), such virtually nil, or too low interfacial tensions to be measured have been reported for droplet-based microfluidic system involving (water/hexadecane) couple containing two kinds of surfactants, and where pearling-like instability readily develops.[37]

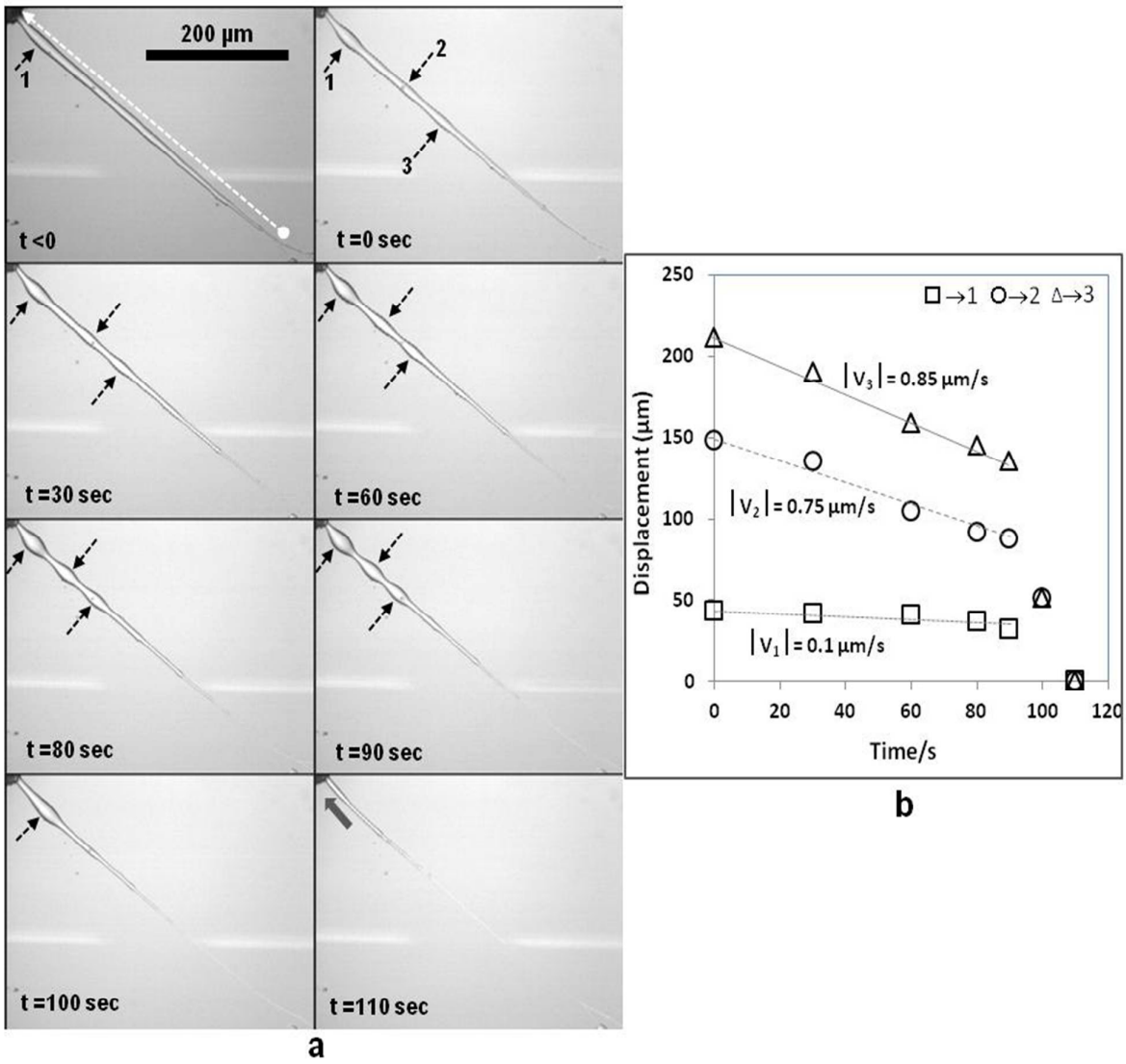

Figure 6: **a**) panel showing the time growth and migration of three nascent pearls (shown by arrows) towards the rim of the macroscopic drop of a DDAB of 0.3 wt%; **b**) displacements and average velocities of the pearls. Although it presents the general feature of the observed propagating pearl-waves, the case treated here was chosen for being the most simple and tractable case. In particular, the measured velocities may differ for other propagating pearls, depending on both their geometric parameters (R_{tub}, R_{pearl}) and attaching conditions: firmly adhering or loosely attached (floating) tubules between the extremities. Note: the terminal acceleration which is observed systematically for any moving pearl arises simply from its merging with another pearl, or with the rim (for the last pearl), driven in that case by the high capillary pressure difference.

Conclusion

In this report, we have studied the wetting behavior of sessile drops of a model double-chain surfactant (DDAB) solution in the so-called "two liquid phase" wetting configuration. Under surrounding alkane oils of the proper chain length, these drops can develop dynamic instabilities that drive the collective growth of membranous tubules. We showed that this wetting-driven tubulation proceeds here by a pinning-induced pulling of embedded structures from the retracting drop edge, rather than by the classical hydrodynamic fingering instability. Besides, we showed that these tubules can also evolve through a pearling fragmentation under quite mild condition (vanishingly low tubule tension), at the difference of most reported pearling destabilization of these membranous tubules that often require external activation sources (optical and photochemical tweezers). This work thus provides a model experimental system for the fundamental study of wetting-driven collective tubulation and pearling in membranous fluid drops, a phenomenon that has so far been seldom investigated and reported in the literature. Naturally, a finer control over the tubules morphology, their stability and related pearling modes and patterns will require more systematic studies (DDAB concentration, surrounding alkane oils). In particular, a relation between the DDAB concentration (structures and viscosity of solution), the lifetime and stability of the tubules vs., pearling would be desired for the full understanding of these phenomena, as strongly suggested here by DDAB drops of 1.5 wt% which show more reproducible and stable tubulation and pearling patterns (Fig. 5) vs., 0.3 wt% DDAB drops. Beyond these fundamental aspects, such parametric studies may open to the possible use of these tubular structures to spatially organize embedded species (nanoparticles, biomolecules) within the tubules and associated pearling patterns that we showed to swell on ageing at higher DDAB concentration (Fig. 5 B). Yet, these results show that the system already contains, virtually, all the potential features for the model study of the collective tubulation, the tubulation morphology as well as their pearling destabilization modes and patterns.

Acknowledgments: The author is grateful to Dr. Laurent Vonna for his help with the final scaling and optimal conversion of the two supporting video movies, and Philippe Kunemann for his kind help for the surface and interface tension measurements of the DDAB solution and DDAB/hexadecane systems.

References

(1) K. B. Migler, *Phys. Rev. Lett*., 2001, **86**, 1023-1026.

(2) Y. Son, N. S. Martys, J. G. Hagedorn and K. B. Migler, *Macromolecules* 2003, **36**, 5825-5833.

(3) F. Brochard-Wyart, F. N. Borghi, D. Cuvelier and P. Nassoy, *Proc. Natl. Acad. Sci.*, 2006, **103**, 7660-7663.

(4) R. M. Hochmuth, N. Mohandas and JR. P. L. Blackshear, *Biophys. J.*, 1973, **13**, 747-762.

(5) T. F. Zhu and J. W. Szostak, *J. Am. Chem. Soc*. 2009, **131**, 5705-5713.

(6) Q. Wang, Marcos V. A. S. Navarro, G. Peng, E. Molinelli, S. L. Goh, B. L. Judson, K. R. Rajashankar and H. Sondermann, *Proc. Natl. Acad. Sci.* 2009, **106**, 12700-12705.

(7) Y. A. Domanov and P. K. J. Kinnunen, *Biophys. J.* 2006, **91**, 4427-4439.

(8) R. Bar-Ziv, T. Tlusty, E. Moses, S. A. Safran and A. Bershadsky, *Proc. Natl. Acad. Sci.* 1999, **96**, 10140-10145.

(9) R. Bar-Ziv and E. Moses, *Phys. Rev. Lett*. 1994, **73**, 1392-1395.

(10) R. Bar-Ziv, T. Tlusty and E. Moses, *Phys. Rev*. *Lett*. 1997, **79***,* 1158-1161.

(11) P. Nelson and T. Powers, *Phys. Rev. Lett*. 1995, **74**, 3384-3387.

(12) T. R. Powers, D. Zhang, R. E. Goldstein and H. A. Stone, *Phys. Fluids* 1998, **10**, 1052-1057.

(13) T. F. Zhu, K. Adamala, N. Zhang and J. W. Szostak, *Proc. Natl. Acad. Sci.* 2012, **109**, 9828-9832.

(14) K. P. Sinha, S. Gadkari and R. M. Thaokar, *Soft Matter* 2013, **9**, 7274-7293.

(15) H. E. Huppert, *Nature* 1982, **300**, 427-429

(16) A. M. Cazabat, F. Heslot, S. M. Troian and P. Carles, *Nature* 1990, **346**, 824-826

(17) P. Carles, S. M. Troian, A. M. Cazabat and F. Heslot, *J. Phys.: Condens. Matter* 1990, **2**, 477-482.

(18) J. Fernandez, P. Kurowski, L. Limat and P. Petitjeans, *Phys. Fluids*, 2001, **13**(11), 3120-3125.

(19) F. Melo, J. F. Joanny and S. Fauve, *Phys. Rev. Lett.* 1989, **63**, 1958-1961.

(20) L. Rayleigh, *Proc. London Math. Soc*. 1878, **10**, 4-13.

(21) F. Caboi and M. Monduzzi, *Langmuir* 1996, **12**, 3548-3556.

(22) S. Mele, A. Khan and M. Monduzzi, *J. Surfactants Deterg.* 2002, **5**, 381-389.

(23) M. Olla, M. Monduzzi and L. Ambrosone, *Colloids and Surfaces A: Physicochem. Eng. Aspects* 1999, **160**, 23-36.

(24) E. Vivares and L. Ramos, *Langmuir* 2005, **21**, 2185-2191.

(25) J. F. A. Soltero, F. Bautista, E. Pecina, J. E. Puig, O. Manero, Z. Proverbio and P. C Schultz, *Colloid Polym. Sci.* 2000, **278**, 37-44.

(26) H. Haidara, L. Vonna andJ. Schultz, *Langmuir* 1998, **14**, 3425-3434.

(27) E. L. Decker and S. Garoff, *Langmuir* 1997, **13**, 6321-6332.

(28) T. Cubaud, P. Jenffer and M. Fermigier, *European Coating Symposium Proceeding*, 2001, 1-4.

(29) A. Bensimon, A. Simon, A. Chiffaudel, V. Croquette, F. Heslot and D. Bensimon, *Science* 1994, **265**(5181), 2096-2098.

(30) J. Zang, Y. Ma, S. Stachura and H. He, *Langmuir* 2005*,* **21**, 4180-4184.

(31) Z. E. Nazari and L. Gurevich, *Beilstein J. Nanotechnol*. 2013, **4**, 72-76.

(32) G. Elender and E. Sackmann, *J. Phys. II France* 1994, **4**, 455-479.

(33) P. G. Saffman and G. I. Taylor, *J. Fluid Mech.* 1958, **245**, 312-329.

(34) T. F. Svitova, Yu. P. Smirnova, S. A.Pisarev and N. A. Berezina, *Colloids Surf. A: Physico-Chem. Eng. Aspects* 1995, **98**, 107-115.

(35) S. K. Mehta, Bhawna, K. K. Bhasin and A. Kumar, *J. Colloid and Interf. Sci.* 2008, **323**, 426-434.

(36) G. H. Sagar and J. R. Bellare, *J. Phys. Chem. B* 2009, **113**, 13805-13810.

(37) M. Hashimoto, , P. Garstecki, H.A. Stone and G. M. Whitesides, *Soft Matter* 2008, **4**, 1403-1413.

Graphical contents entry

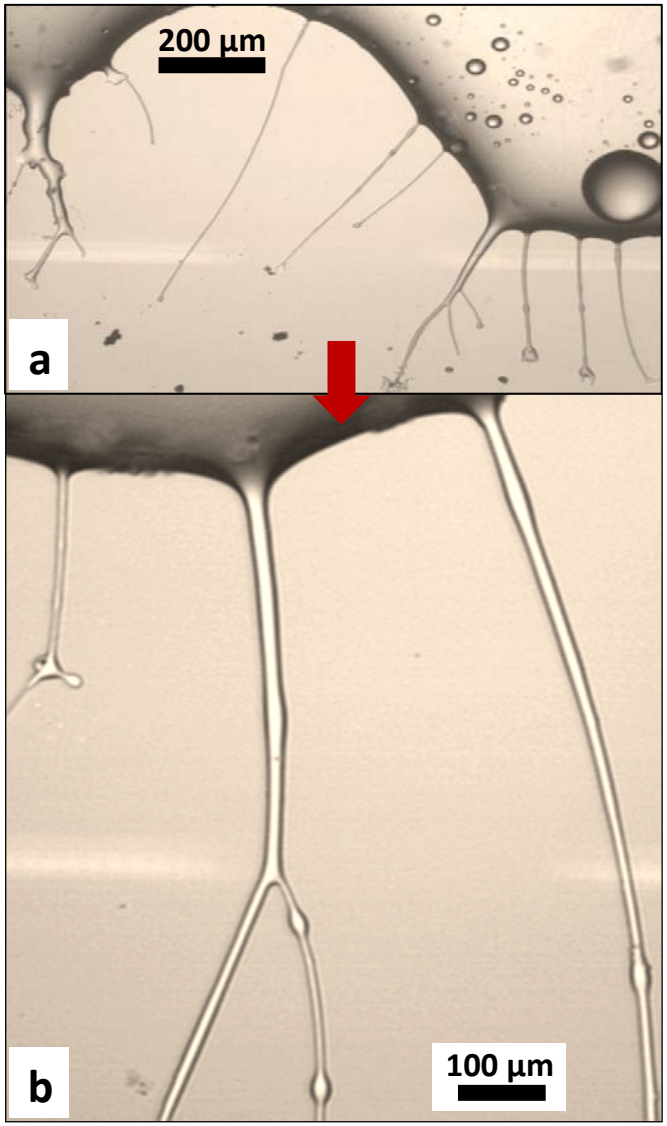

Wetting-driven collective tubulation and pearling patterns in a sessile drop of aqueous DDAB surfactant solution (3 wt %), surrounded by an alkane oil. (color online).